Crack Propagation Model from Coupled Atomistic-Continuum Simulations

Somnath Ghosh

Graduate Students: Jiaxi Zhang and Subhendu Chakraborty

Departments of Civil, Mechanical and Materials Science &Engineering

Johns Hopkins University

Baltimore, USA

Acknowledgements: National Science Foundation

NIST Workshop on Atomistic Simulations for Industrial Needs

Gaithersburg, MD

August 2, 2018

Modeling Fatigue and Failure in Crystalline Materials

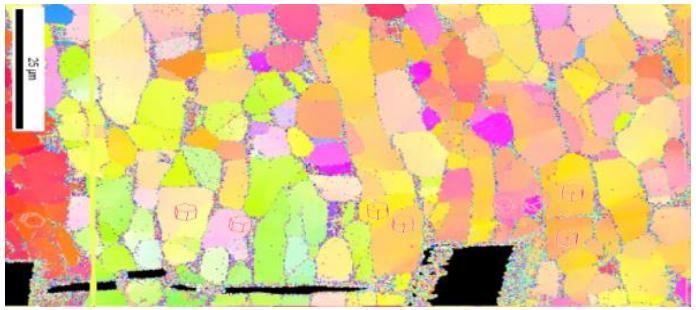

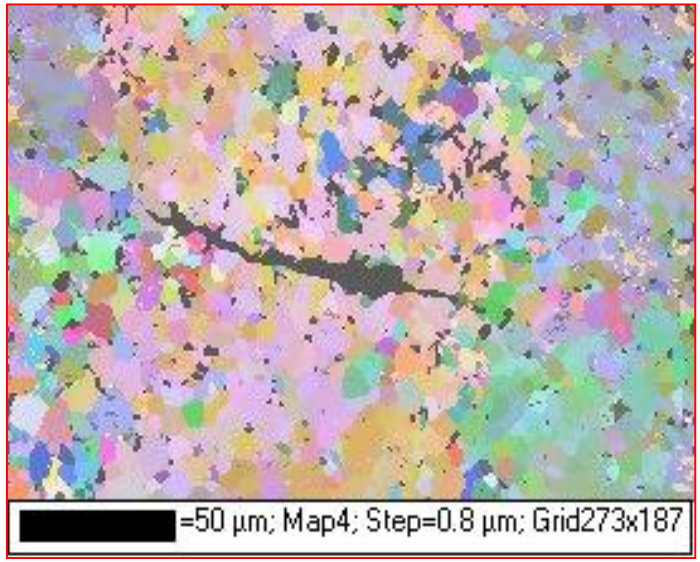

Ti-6242

Williams, Sinha, Mills, Bhattacharjee, (2006)

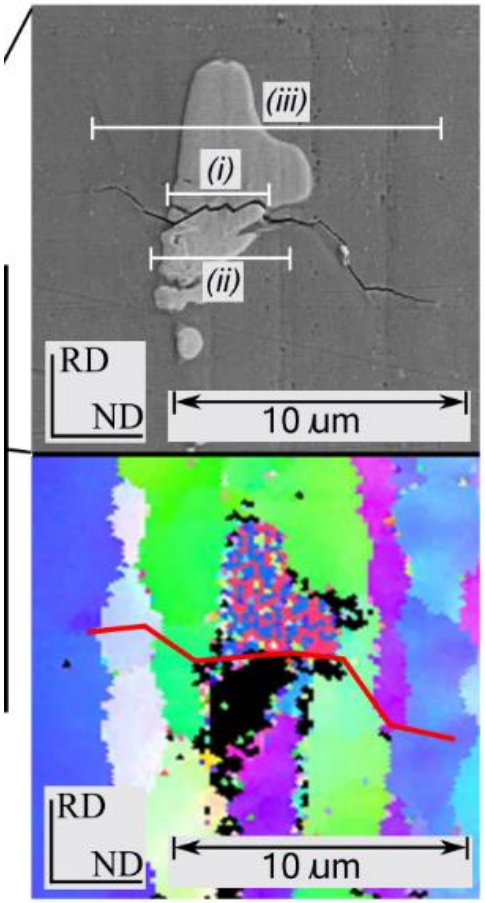

Al- 7075-T651

Hochhalter et al. (2010)

Short and Long Crack Propagation in Polycrystalline Microstructures

Stage I – Short Crack Growth

- Plastic zone at grain scale
- Strong microstructure dependence, grain boundary, dislocation structure, slip , etc.

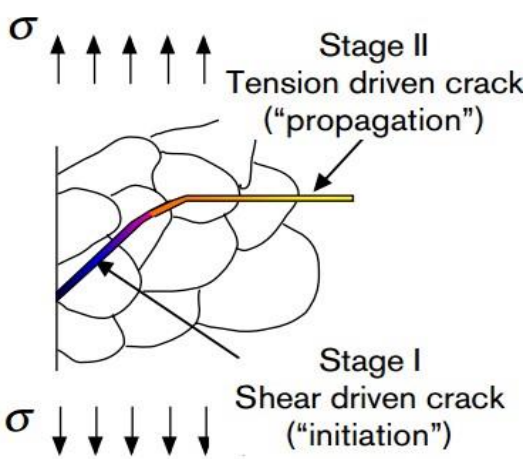

http://fcp.mechse.illinois.edu

Stage II – Long Crack Growth

- Insensitive to microstructure
- Paris' Law

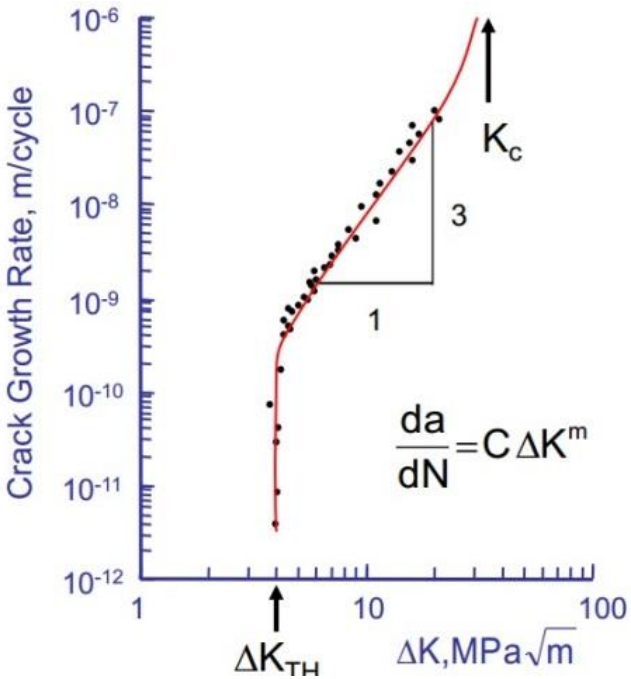

Short Crack Evolution
Cohesive zone models

Separation between material surfaces resisted by cohesive tractions

Needleman (1990), Ortiz and Pandolfi (1999), Park Paulino, Roesler (2009)

Spearot, McDowell (2004), Yamakov, Saether E, Glaessgen E (2008)

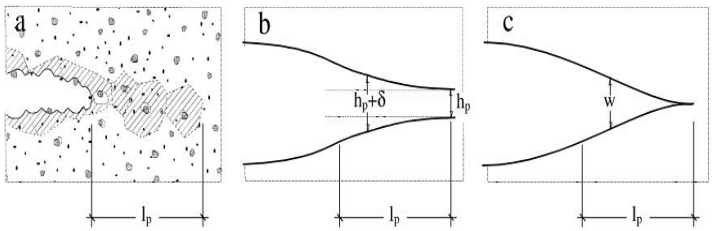

Process Zone

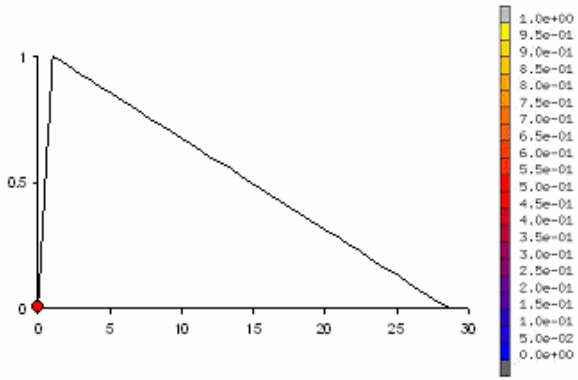

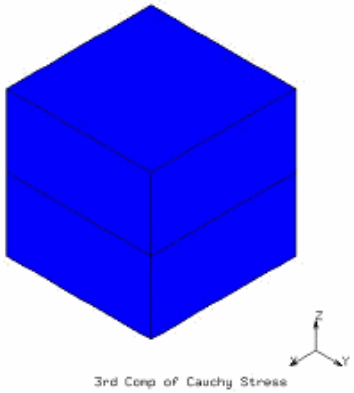

- Parameters of cohesive potential are typically calibrated by experiments
- Interaction between crack growth and local plasticity evolution which affected by the local microstructure is not included

Phase-Field Modeling

Continuous Auxiliary Field to Approximate Sharp Crack Discontinuities.

Clayton and Knap (2015),
Miehe, Hofacker, and Welschinger (2010),
Ambati, Gerasimov, and Lorenzis, (2015).

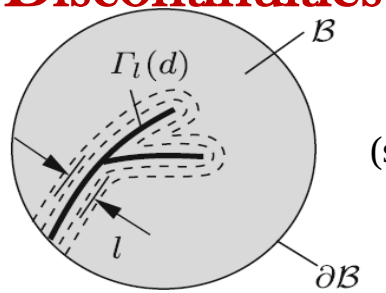

(s)

$$s(x) = e^{-|x|/l_c}$$

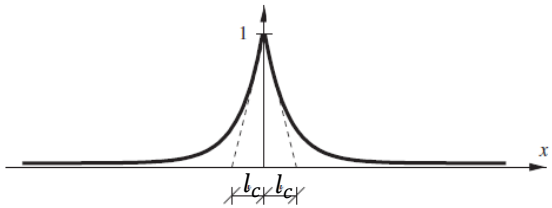

Diffused crack

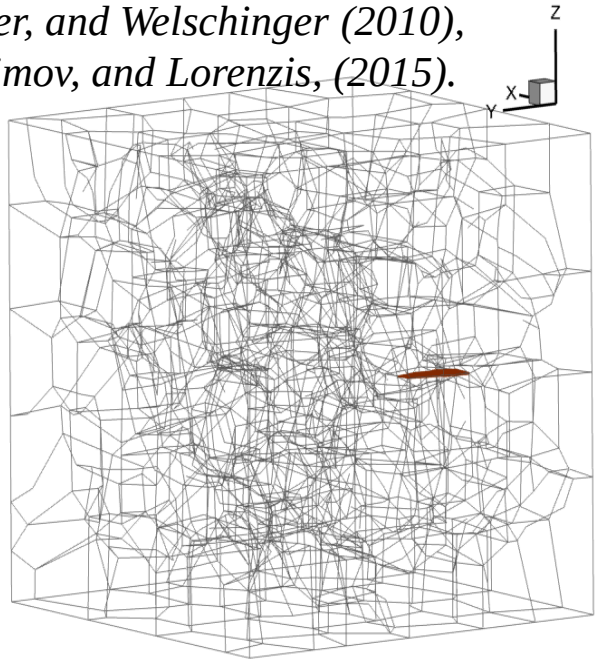

s is the phase field variable (order parameter):
$\boldsymbol{s} \in [\mathbf{0}, \mathbf{1}]$; $\boldsymbol{s} = \mathbf{0}$ perfect solid; $\boldsymbol{s} = \mathbf{1}$ fully cracked

Helmholtz stored energy and crack dissipation are modeled with phase field:

Stored free energy: $\Psi = \Psi^e(\boldsymbol{E}^e, s) + \Psi^d(\boldsymbol{\eta}, s) + \Psi^f(s, \nabla s)$

Dissipation rate: $\dot{D} = W^{ext} - \left(\dot{\Psi}^e + \dot{\Psi}^d + \dot{\Psi}^f\right)$

Energy functionals are typically not rooted in the atomistic source of the fracture region

Objective of this Study

- Upscaling of variables from atomic-scale molecular dynamics simulations in a self-consistent model.
- Develop physics-based, integrated framework of crack evolution and deformation models for crystalline materials that can be used in conjunction with crystal plasticity finite element models.

Sequence of Steps in Building the Model

- **Characterizing mechanisms in atomistic simulations**
  (Zhang, Ghosh JMPS, 2013)

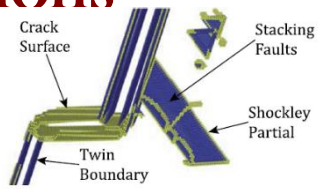

- **Self-consistent coupled atomistic-continuum model**
  (Zhang, Chakraborty, Ghosh IJMCE 2017, Ghosh Zhang IJF 2017)

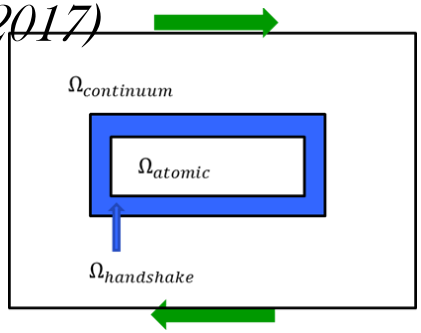

- **Crack propagation using coupled model**
- **Hyperdynamics for time-scale acceleration**
  (Chakraborty, Zhang, Ghosh CMS 2016, Chakraborty, CMS Ghosh 2018)
- **Extracting crack growth models, e.g. phase field energies**
  (Ghosh Zhang IJF 2017, Chakraborty, CMS Ghosh 2018)

I. Atomistic Simulations with Mechanism Characterization and Quantification

MD simulation provides tools to capture deformation mechanisms which dominate crack tip plasticity and affect crack propagation process.

J. Zhang and S. Ghosh, JMPS, Vol. 61, 1670-1690, 2013

Mechanism	Dislocation	Twinning	Crack/void
Descriptor	Core structure	Lattice rotation	Nearest neighbors
Characterization	CNA		
Method	DXA	Deformation gradient	Equivalent ellipse
Quantifying variable	Total length		Crack length
	Total density	Volume fraction	Crack opening

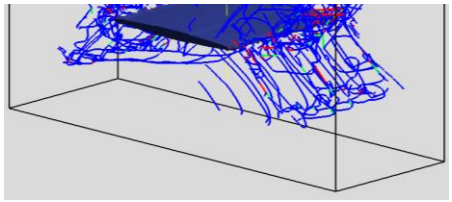

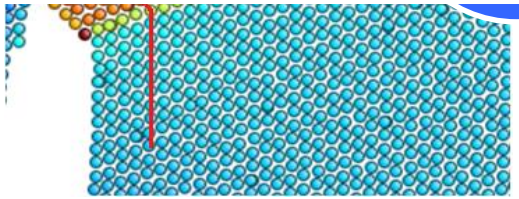

I. Characterization and Quantification of Mechanisms in Molecular Simulation

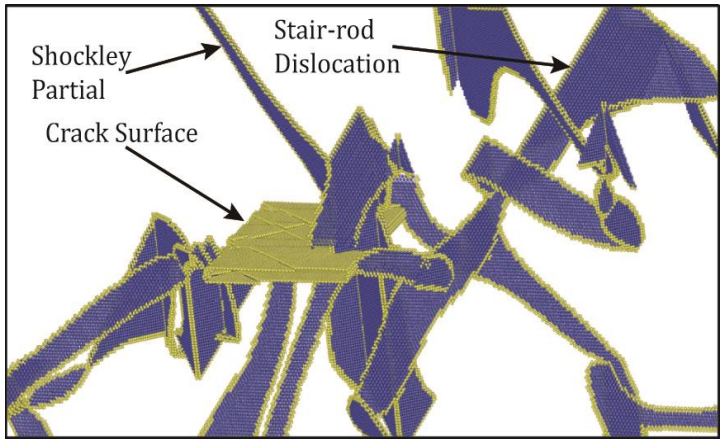

Dislocation Extraction (DXA)

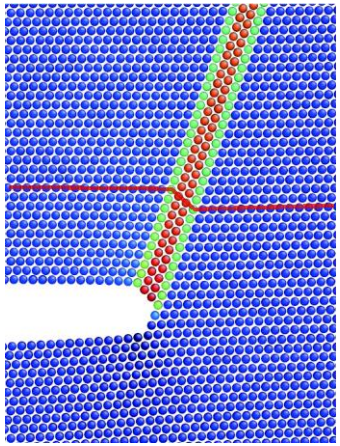

Deformation gradient for twins

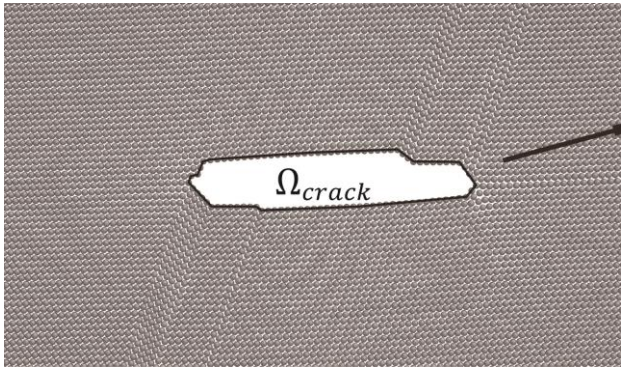

Crack surface

Dislocation	CNA, DXA	Dislocation density, Burgers vector
Twin	Deformation gradient	Twin volume fraction
Crack surface	Equivalent ellipse	Crack length, opening

A MD Model to Study Evolution of Crack and Associated Mechanisms

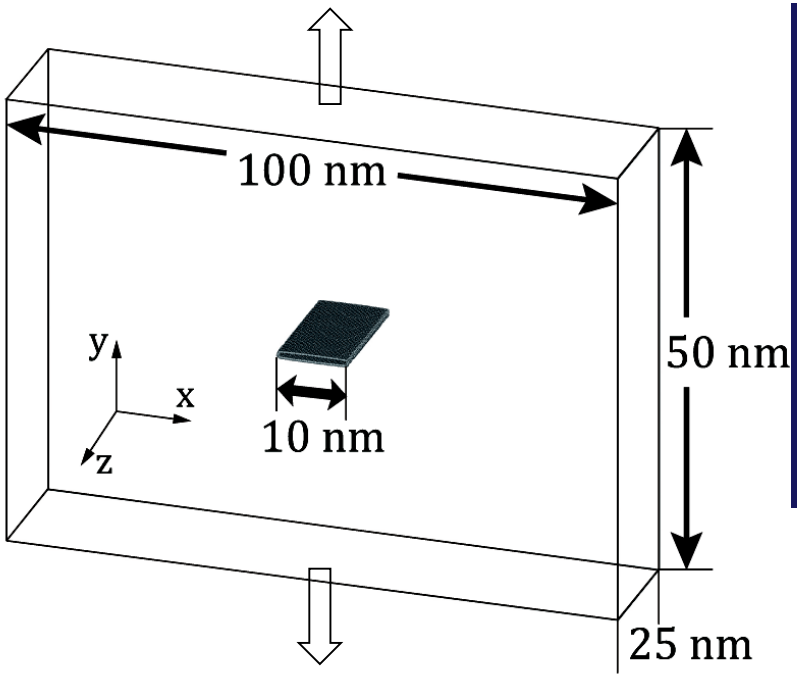

- Nickel Single Crystal: MEAM potential
- NPT ensemble ~1K
  100 nm x 60nm x 25nm(10 million atoms)
  Periodic boundary condition
  Initial small crack in the center
  Tensile loading, strain controlled
  Strain-rate ~ 10^7 s^{-1}

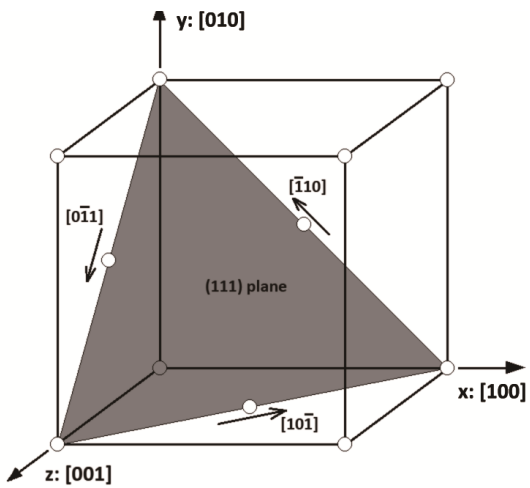

1. Orientation 1: $x \rightarrow [\bar{1}10]$, $y \rightarrow [111]$, $z \rightarrow [11\bar{2}]$
2. Orientation 2: $x \rightarrow [11\bar{2}]$, $y \rightarrow [111]$, $z \rightarrow [1\bar{1}0]$

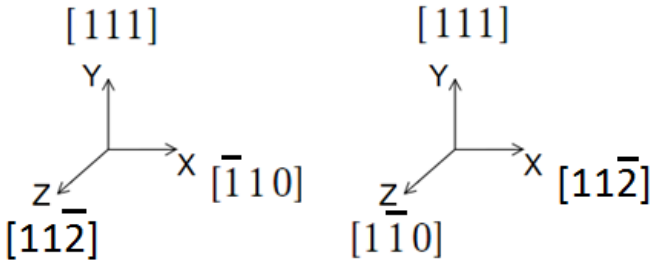

A. Evolution of Deformation Mechanisms

Orientation 1: $x \rightarrow [\bar{1}10]$, $y \rightarrow [111]$, $z \rightarrow [11\bar{2}]$

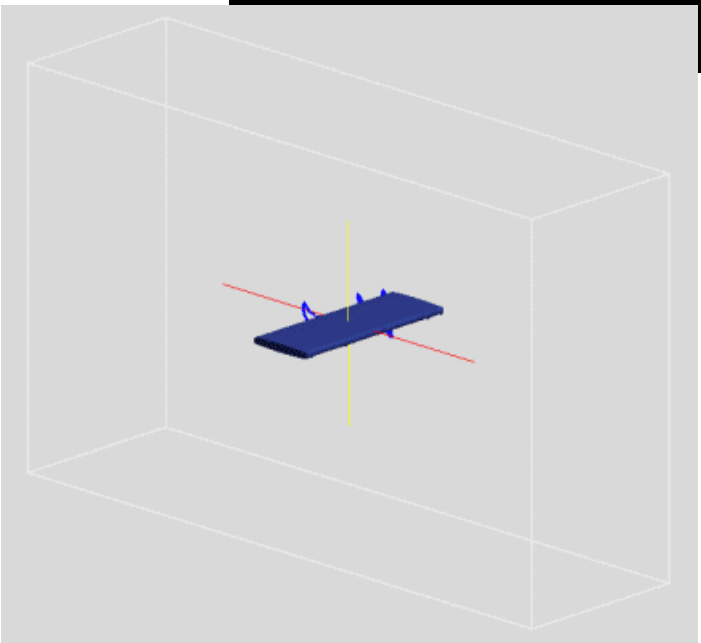

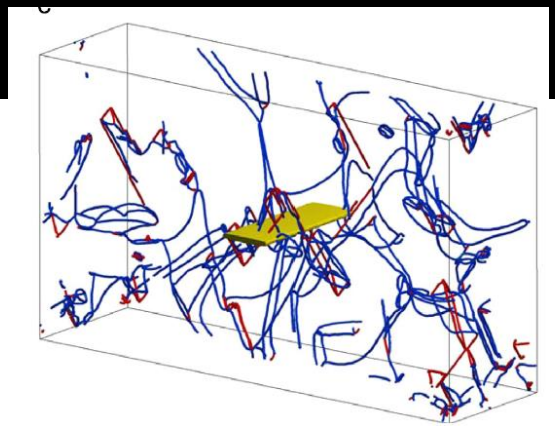

Stabilized Dislocation Structure at 2.7% Strain.

Dislocation segments colored by magnitude of Burgers vector

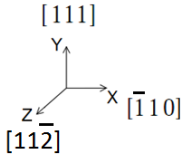

$$blue: b = \frac{1}{6}\langle 112 \rangle \{111\}$$

$$red: b = \frac{1}{6}\langle 110 \rangle \{111\}$$

$$green: b = \frac{1}{3}\langle 100 \rangle \{111\}$$

- After critical stress, partial dislocation emission from crack-tip slip caused by dislocation gliding blunts crack tip and reduces stress concentration
- No brittle crack propagation by bond cleavage
- Crack evolution for this orientation is governed by hydrostatic strain and slip, resembling void growth
- Formation of dislocation junctions, junction length takes 30% of total length

B. Evolution of Deformation Mechanisms

Orientation 2: $x \rightarrow [11\bar{2}]$, $y \rightarrow [111]$, $z \rightarrow [1\bar{1}0]$

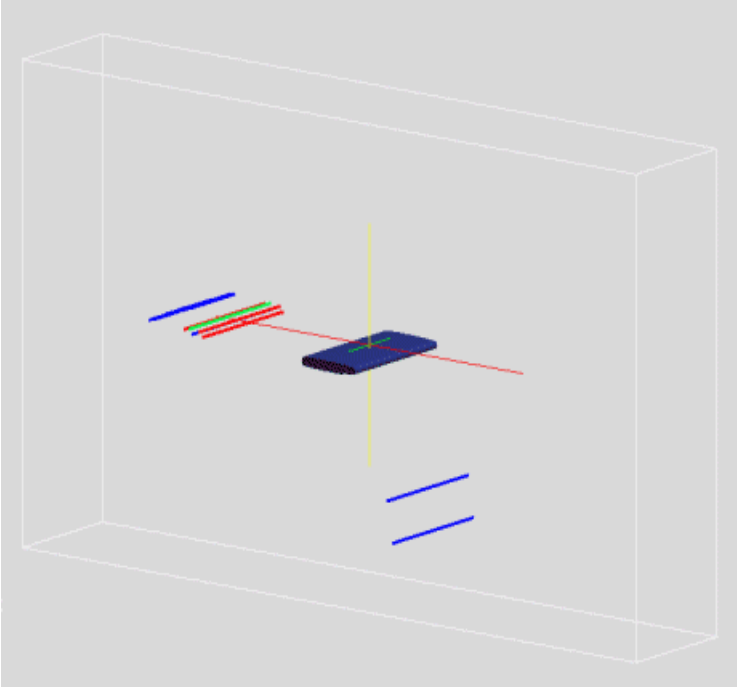

- Deformation mechanisms divided into two categories, (i) twin partials contributing to slip (ii) dislocation motion contributing to slip.
- Twins formed at crack tip by sequential leading partial dislocations nucleated on adjacent {111} plane
- All twin partials are *edge* partials with no cross-slip
- At ~ 3.3% tensile strain, dislocation loop starts to emit from the crack tip, gliding in the {111} plane.
- Twin boundaries impede dislocation motion, similar to dislocation junction

Dislocations interact with twin boundary forming stair-rod dislocations

Dislocation segments colored by magnitude of Burgers vector

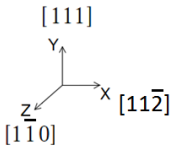

blue: $\boldsymbol{b_1} = \frac{1}{6}\langle 112\rangle\{111\}$

red: $\boldsymbol{b_2} = \frac{1}{6}\langle 110\rangle\{111\}$

green: $\boldsymbol{b_3} = \frac{1}{3}\langle 100\rangle\{111\}$

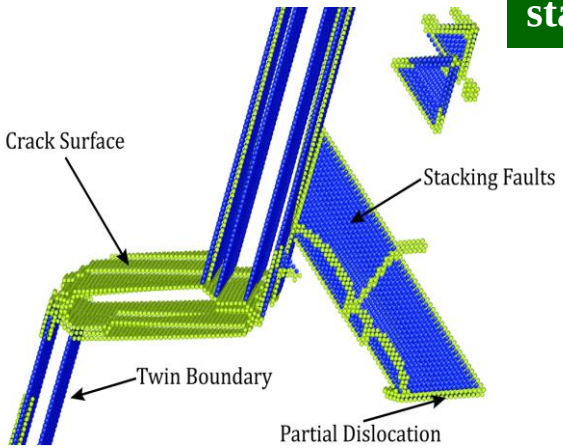

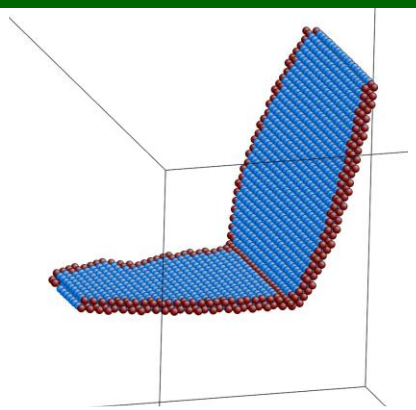

Energy Partitioning Associated with Deformation Mechanisms

Lattice Orientation 1: $x \to [\bar{1}10]$, $y \to [111]$, $z \to [11\bar{2}]$

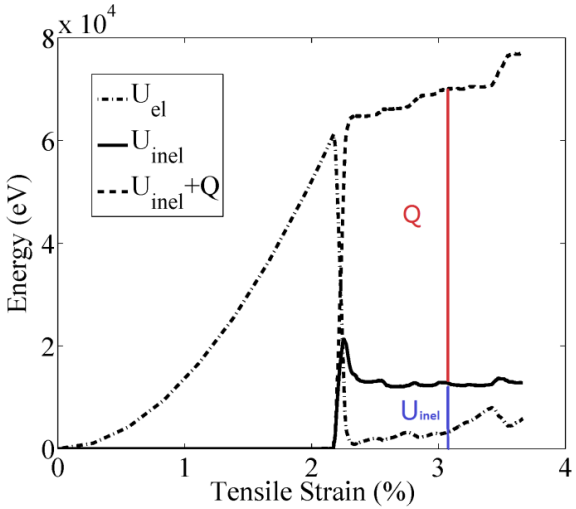

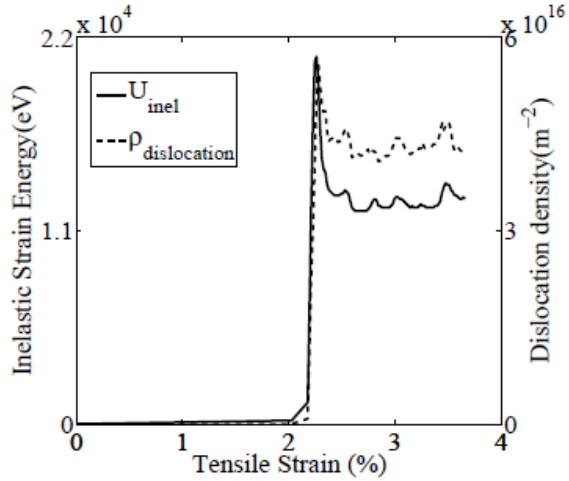

$$dW = dU_{el} + dU_{inel} + dQ$$

Dislocation dominated

$$\mu_{dislocation} \sim 0.8$$

Energy evolution profile can suggest the deformation mechanism!

Lattice Orientation 2: $x \to [11\bar{2}]$, $y \to [111]$, $z \to [1\bar{1}0]$

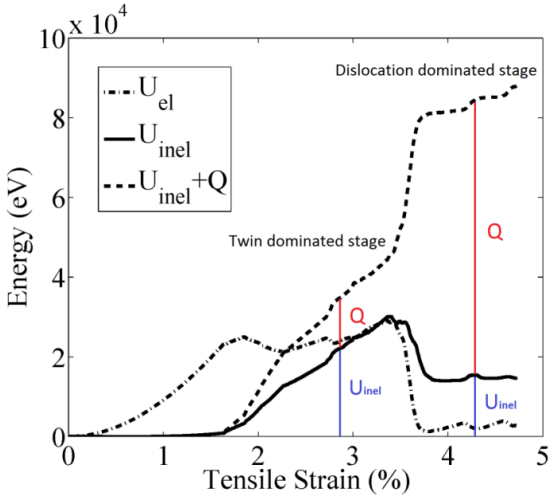

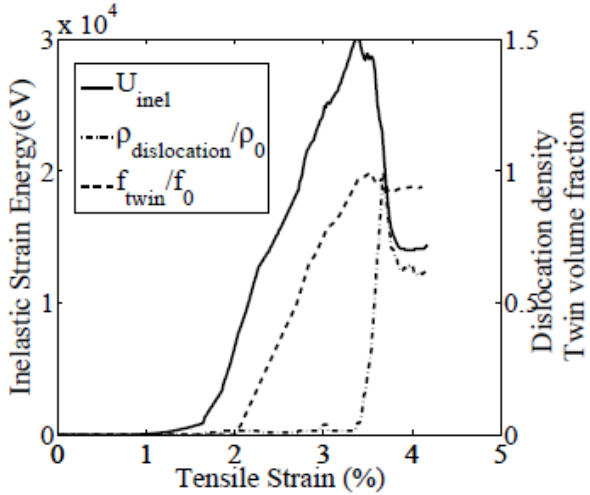

Twin first then dislocation

$$\mu_{twin} \sim 0.4$$

Heat transfer coefficient

$$\mu \triangleq \frac{Q}{Q+U_{inel}}$$

II. A Coupled Concurrent Model

- ❑ Finite temperature
- ❑ Non-equilibrium simulation
- ❑ Should handle dislocation transfer

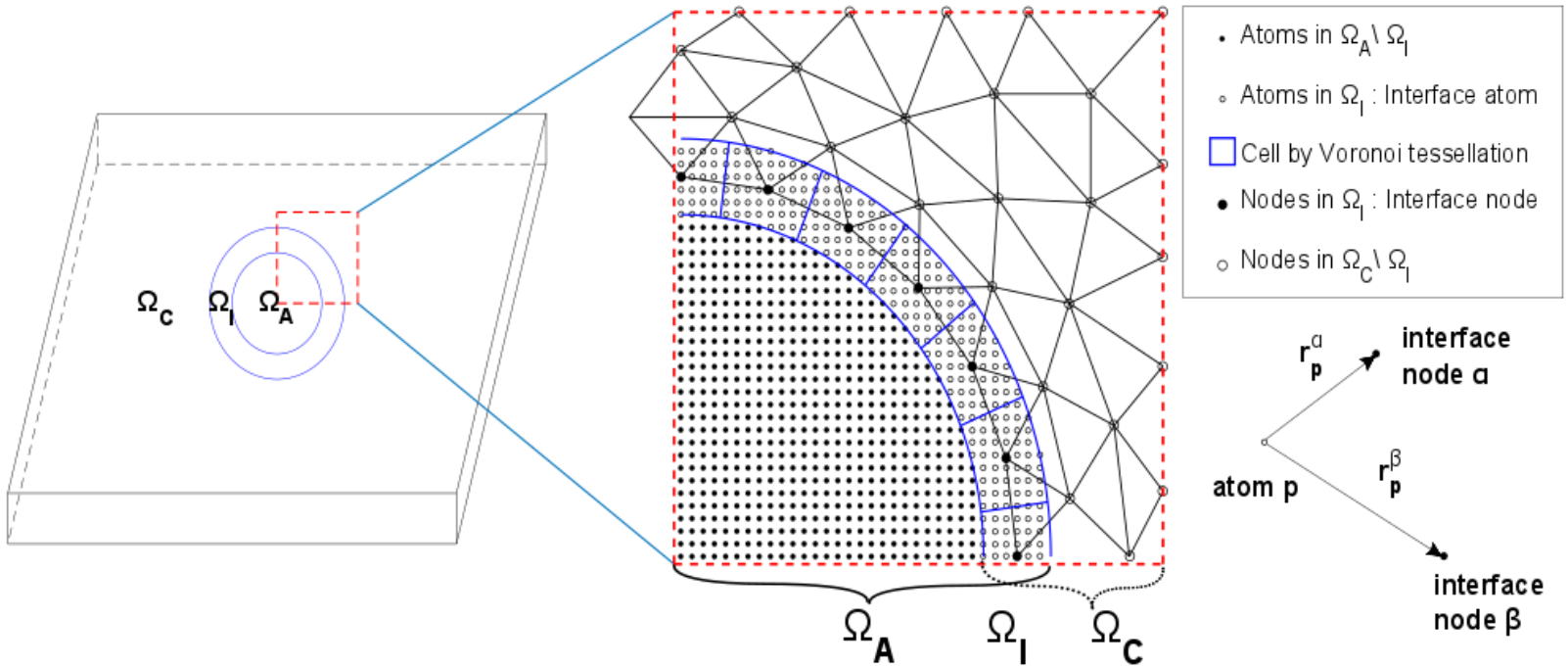

Zhang, Chakraborty and Ghosh (2017).
Ghosh and Zhang (2017).

Numerical Implementation

Molecular Dynamics

Velocity Verlet and NVE ensemble (LAMMPS)

Solve for displacement field and its time average for any atom j in handshake region

$$u_i(t), \langle u_i(t) \rangle$$

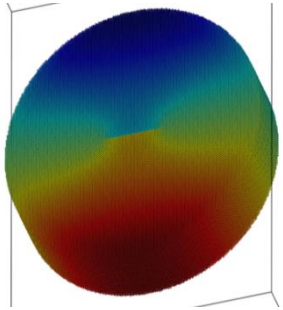

Handshake region

Boundary nodes displacement on node I

$$u_I^C = \sum_j^{m_I} w_j \langle u_j^A \rangle$$

Boundary atoms external force on atom j

$$f_j^{\text{ext}} = w_j R_I^C$$

FEM

Quasi-static equilibrium configuration

Solve for reaction force of any boundary node I with displacement B.C.

$$R_I$$

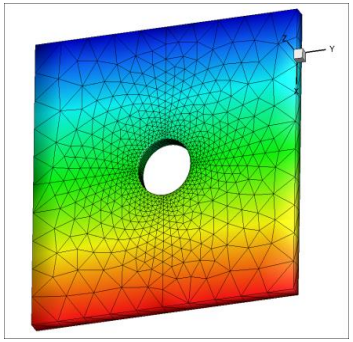

Concurrent Formulation

Equilibrium equations for the quasi-static problem are obtained by minimizing the total potential energy functional of the system.

$$\Delta\Pi_{tot} = \Delta\Pi_C + \Delta\Pi_A + \Delta\Pi_I$$

$$\Delta\Pi_C = \int_{\Omega_C} \boldsymbol{\sigma} : \Delta\boldsymbol{\epsilon} dV - \int_{\partial\Omega_C} \boldsymbol{t} \cdot \Delta\boldsymbol{u}^C dA = \{\boldsymbol{f}_{\text{C-int}} - \boldsymbol{f}_{\text{C-ext}}\} \cdot \{\Delta\boldsymbol{u}^C\}$$

$$\Delta\Pi_A = \sum_{p\in\Omega_A} \Delta\Phi_p(\bar{\boldsymbol{r}}) - \sum_{p\in\Omega_A} \boldsymbol{f}^p_{\text{A-ext}} \cdot \Delta\bar{\boldsymbol{r}}_p$$

$$\Delta\Pi_I = \sum_{\beta\in\Omega_I} \boldsymbol{\lambda}_\beta \cdot \boldsymbol{C}_\beta$$

Compatibility Constraint

$$C_\beta(\Delta\boldsymbol{u}^C, \Delta\boldsymbol{u}^A) = \Delta\boldsymbol{u}^C_\beta - \sum_{p\in G_\beta} w_p \cdot \Delta\boldsymbol{u}^A_p = 0 \quad \forall\beta \in \Omega_I$$

Concurrent Formulation

Equilibrium configuration of the coupled-concurrent system

$$\frac{\partial \Delta \Pi_{tot}}{\partial \Delta u^i_\alpha} = f^i_\alpha = \begin{cases} (f^i_\alpha)_{\text{int}} - (f^i_\alpha)_{\text{ext}} + \lambda^i_\alpha & \text{for node } \alpha \in \Omega_I \\ (f^i_\alpha)_{\text{int}} - (f^i_\alpha)_{\text{ext}} & \text{for node } \alpha \in \Omega_C \backslash \Omega_I \end{cases} = 0 \tag{4a}$$

$$\frac{\partial \Delta \Pi_{tot}}{\partial \Delta \bar{r}^i_p} = f^i_p = \begin{cases} \frac{\partial \Delta \Phi(r)}{\partial \Delta \bar{u}^i_p} - (f^i_p)_{\text{ext}} - w_p \lambda^i_\alpha & \text{for atom } p \in G_\alpha \text{ in } \Omega_I \\ \frac{\partial \Delta \Phi(r)}{\partial \Delta \bar{u}^i_p} - (f^i_p)_{\text{ext}} & \text{for atom } p \in \Omega_A \backslash \Omega_I \end{cases} = 0 \tag{4b}$$

Compatibility Constraint

$$(\lambda^i_\alpha)^C + (\sum_{p \in G_\beta} w_p \lambda^i_\alpha)^A = 0$$

Numerical Implementation

Continuum Model

$$\{\boldsymbol{f}^C_{\text{int}}(t+\Delta t)\} = \{\boldsymbol{f}^C_{\text{int}}(t)\} + \{\Delta \boldsymbol{f}^C_{\text{int}}\}$$
$$\{\boldsymbol{f}^C_{\text{ext}}(t+\Delta t)\} = \{\boldsymbol{f}^C_{\text{ext}}(t)\} + \{\Delta \boldsymbol{f}^C_{\text{ext}}\}$$
$$\{\boldsymbol{\lambda}(t+\Delta t)\} = \{\boldsymbol{\lambda}(t)\} + \{\Delta \boldsymbol{\lambda}\}$$

$$\begin{bmatrix} \boldsymbol{K}^{C-II} & \boldsymbol{K}^{C-IU} \\ \boldsymbol{K}^{C-UI} & \boldsymbol{K}^{C-UU} \end{bmatrix}^k \begin{Bmatrix} \Delta \boldsymbol{U}^{C_I} \\ \Delta \boldsymbol{U}^{C_U} \end{Bmatrix}^k - \begin{Bmatrix} 0 \\ \Delta \boldsymbol{f}^{C_U}_{\text{ext}} \end{Bmatrix}^k + \begin{Bmatrix} \Delta \boldsymbol{\lambda} \\ 0 \end{Bmatrix}^k = 0$$

MD Model

$$m_p \ddot{\boldsymbol{u}}_p = \boldsymbol{f}_p$$

$$\boldsymbol{f}^I_p = -\boldsymbol{\nabla}\Phi + w_p \boldsymbol{\lambda}_\beta + \boldsymbol{f}^p_{\text{A-ext}} - \gamma m_p \dot{\boldsymbol{r}}_p + \sqrt{2\gamma K_B \theta m_p} R(t)$$

In addition to inter-atomic interactions, atoms also experience forces due to atom-node interaction. Damping is applied to this region for maintaining temperature and elastic waves are suppressed by using a Langevin thermostat.

Self-Consistency → Non-linearity and Non-locality

Non-linear inter-atomic interactions

$$\Phi(\epsilon) = \frac{1}{2!} c_{ijkl}\epsilon_{ij}\epsilon_{kl} + \frac{1}{3!} c_{ijklmn}\epsilon_{ij}\epsilon_{kl}\epsilon_{mn}$$

Comparing average deformation gradient at interface of atomistic and continuum

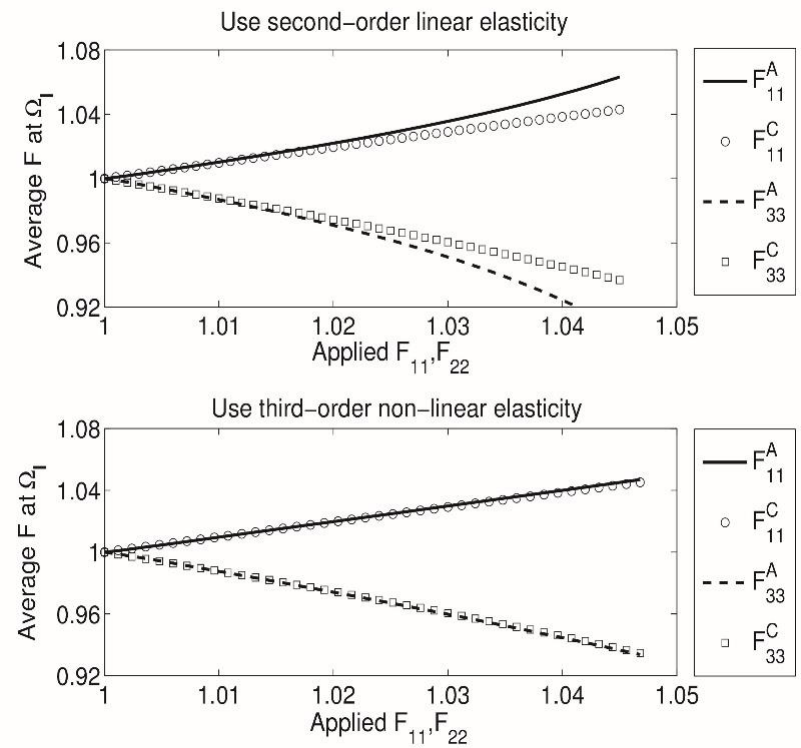

Non-local inter-atomic interactions

$$\sigma_{ij} = c_{ijkl}(\epsilon_{kl} - l^2\nabla^2\epsilon_{kl})$$

Near crack tip, the stress and strain to evaluate the length scale parameter

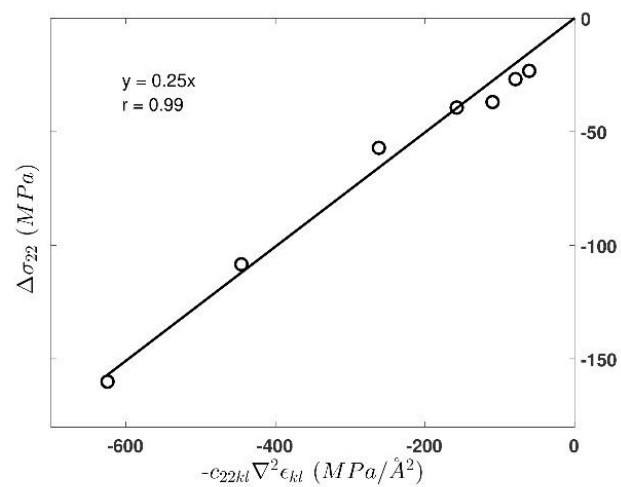

Slope corresponds to l^2, it is found for Nickel with EAM potential used, $l \approx 0.5$Å

III. Time Acceleration of Atomistic Domain Using Strain Boost Hyperdynamics

[1] S. Hara and J. Li, PRB 82, 184114 (2010)

Biased system potential,

$$V_b = V(r) + \Delta V(r)$$

Boost potential,

$$\Delta V(r) = \frac{F\left(\eta_{\max}^{Mises}\right)}{N_b} \sum_{i=1}^{N_b} \delta V_i\left(\eta_i^{Mises}\right)$$

$$F\left(\eta_{\max}^{Mises}\right) = 1 - \left(\frac{\eta_{\max}^{Mises}}{q_c}\right)^2 \quad if \;\; \eta_{\max}^{Mises} \le q_c$$

$$= 0 \quad if \;\; \eta_{\max}^{Mises} \ge q_c$$

$$\delta V_i = V_{\max}\left[1 - \left(\frac{\eta_i^{Mises}}{q_c}\right)^2\right]$$

$$\text{Boost Factor} = \exp\left(\frac{\Delta V}{K_b T}\right)$$

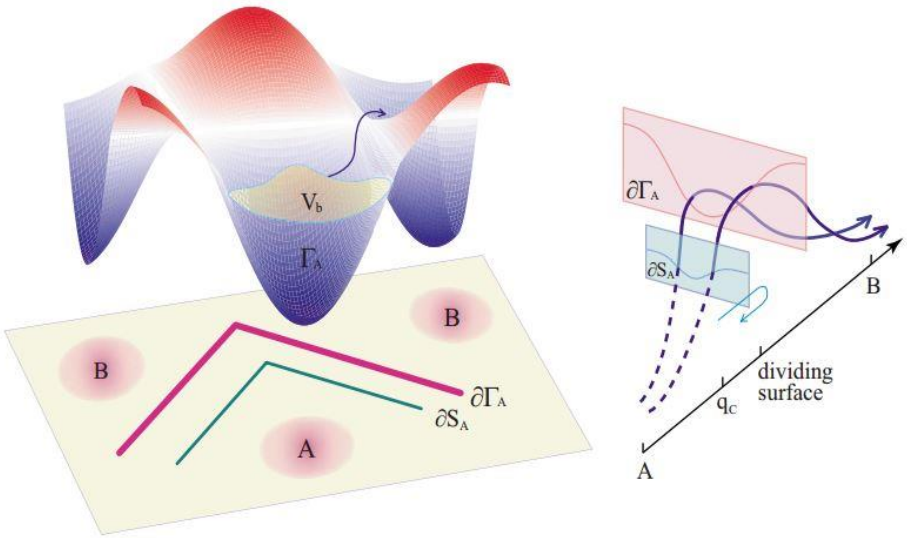

- η_i^{Mises} is Von-Mises strain of atom 'i', calculated from least square based atomic deformation gradient.
- N_b is total number of atoms to be boosted.
- V_{max} and q_c are material parameters.

Determination of Strain Boost Hyperdynamics Parameters

$$\delta V_i = V_{\max}\left[1-\left(\frac{\eta_i^{Mises}}{q_c}\right)^2\right]$$

- "q_c" corresponds to critical value of "η_{max}" at the onset of transition.
- V_{max} scales with the energy barrier.
- MD simulation is conducted for a small sample to calibrate "q_c" and "V_{max}".

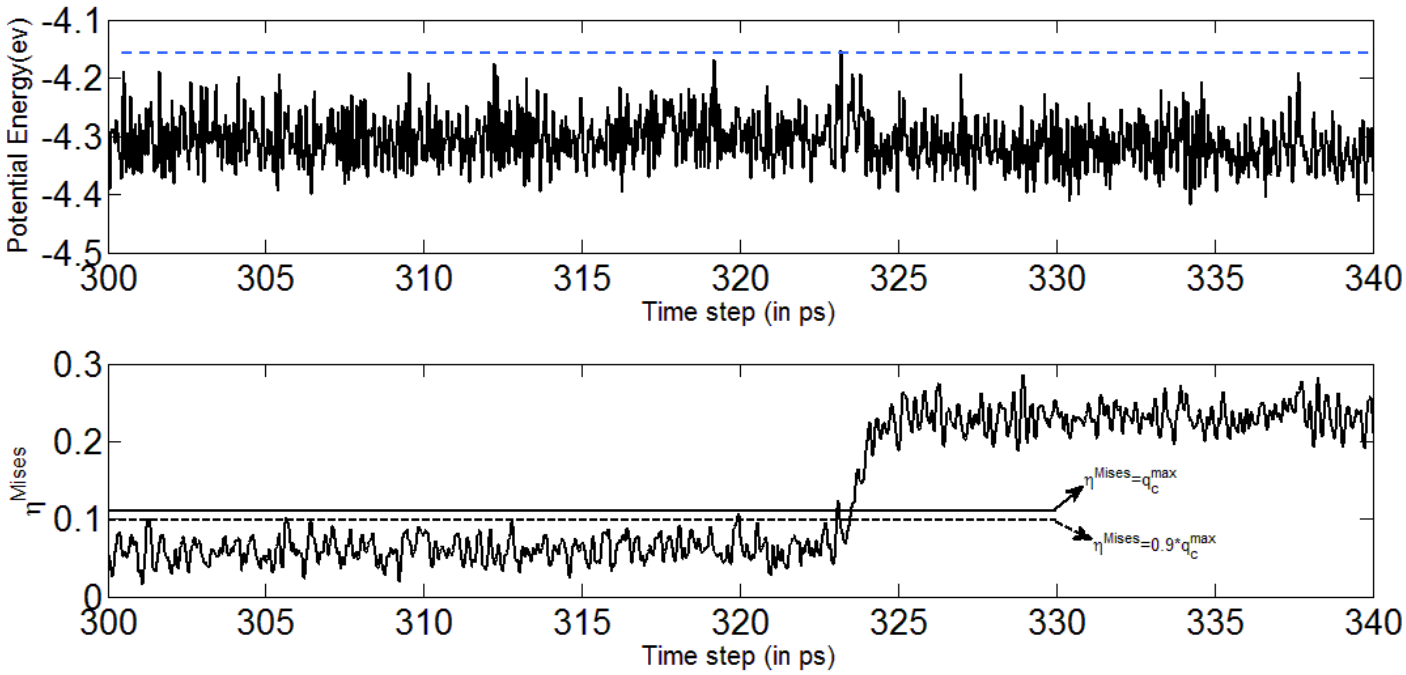

Determination of Boost Region

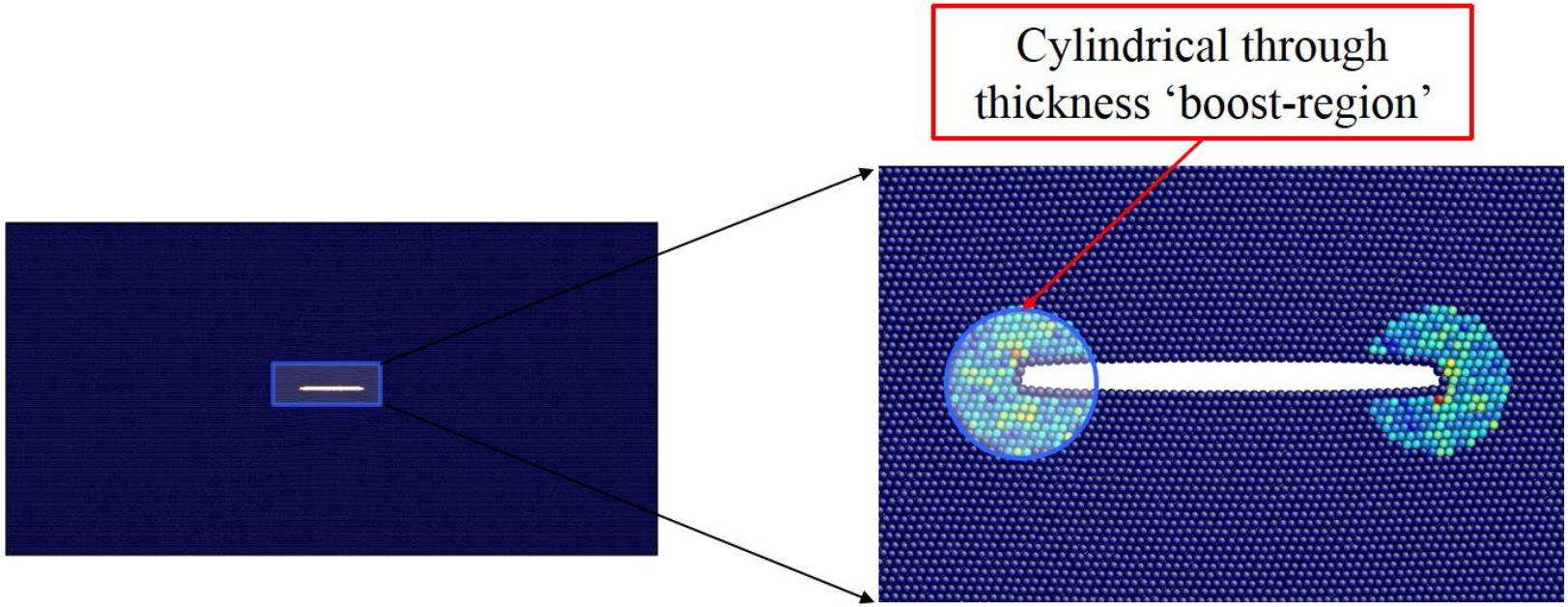

- Extra computational cost scales with number of atoms in boost region.
- Boost region should include all the critical atoms from where nucleation is likely to happen.
- New atoms are tagged adaptively as 'to be boosted' during the simulation.

Simulation Results – Orientation 1

Lattice Orientation 1 : $x \rightarrow [\bar{1}10]$ $y \rightarrow [111]$ $z \rightarrow [11\bar{2}]$

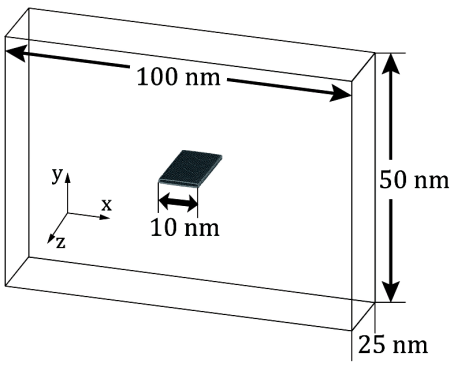

- Less number of dislocations nucleate at low strain rate.
- Reduction in number of dislocation increases the free path for dislocation to glide before it interacts with other dislocation forming immobile junction (stair-rod dislocation).

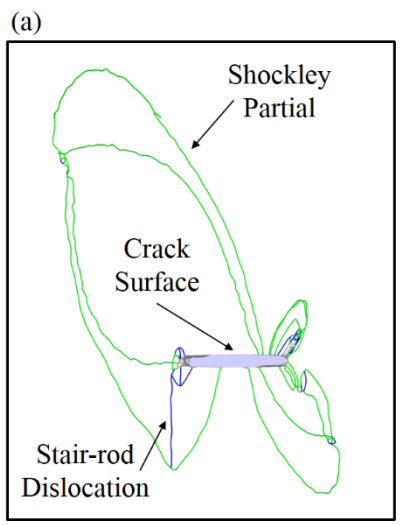

Conventional MD with $\dot{\varepsilon} = 2 * 10^7/sec$

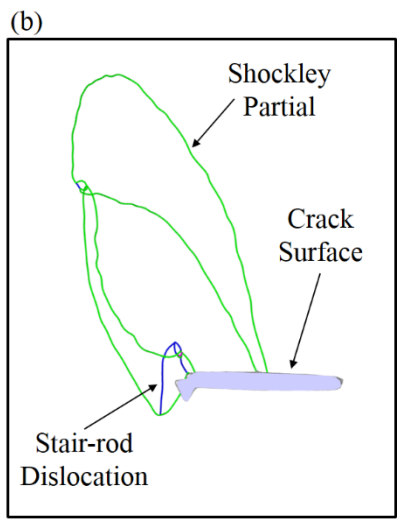

Hyperdynamics with $\dot{\varepsilon} = 10^4/sec$

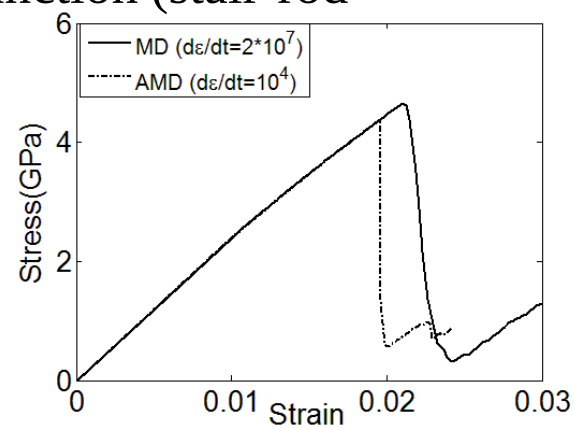

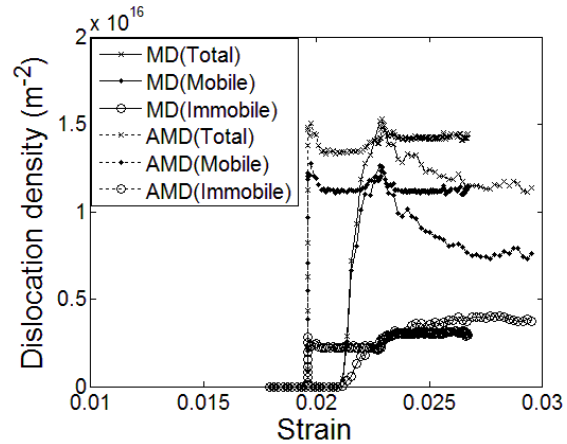

Simulation Results – Orientation 2

Lattice Orientation 2 : $x \rightarrow [11\bar{2}]$ $y \rightarrow [111]$ $z \rightarrow [1\bar{1}0]$

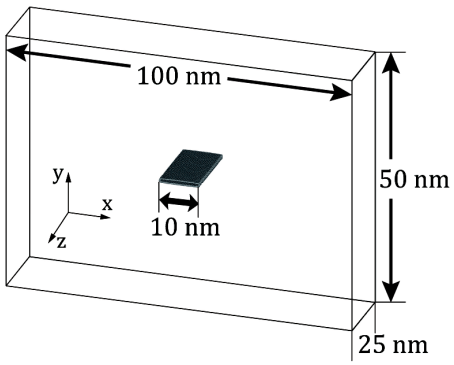

- At high strain rate nucleation of successive leading partials in parallel slip plane is preferred forming a **micro twin band**.
- At low strain rate leading partial is followed is by a trailing partial in the same slip plane forming a **full dislocation**.

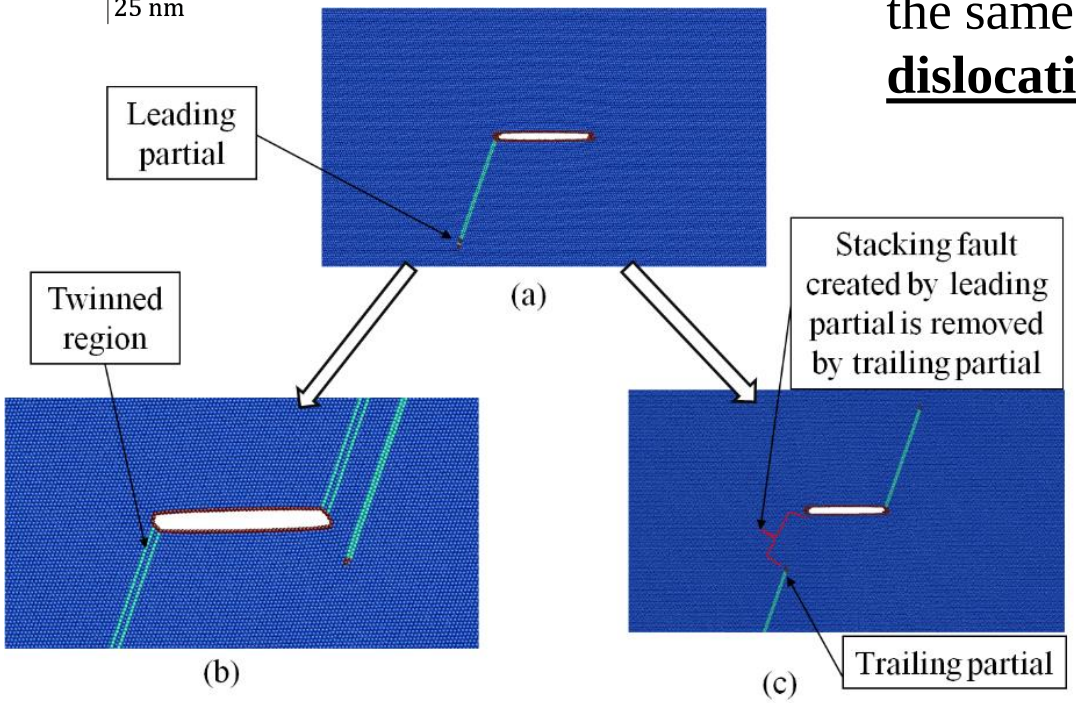

Ref. *S. Chakraborty, J. Zhang and S. Ghosh, Computational Material Science, 121:23-34(2016).*

Time-Scale Bridging in Coupled Concurrent Simulation

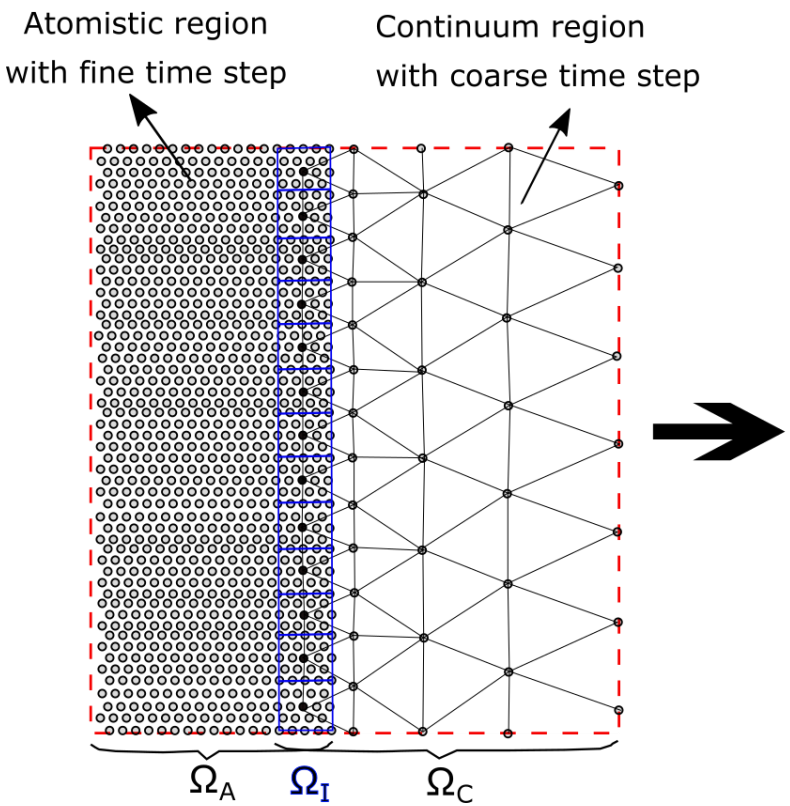

At the end of each load increment both atomistic and continuum regions are in same time scale and equlibriated

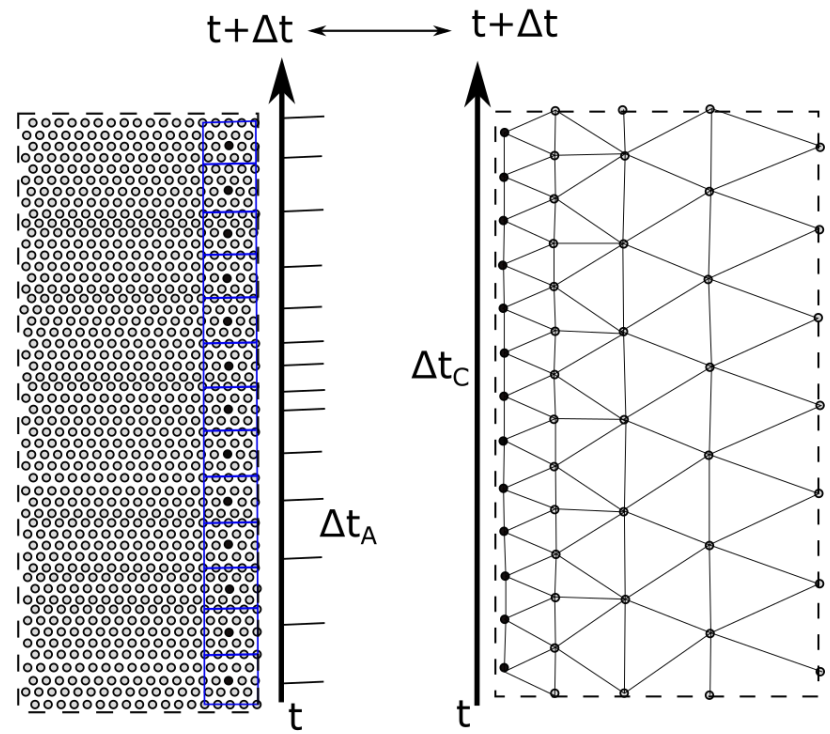

$$\Delta t_A = \Delta t_{MD} * \exp\left(\frac{\Delta V}{K_b T}\right)$$

Crack Propagation Rate at Low Strain Rates

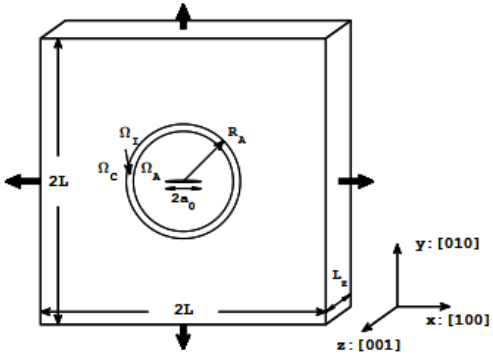

- 2L=200nm.
- R=32nm.
- $2a_O$=20nm.

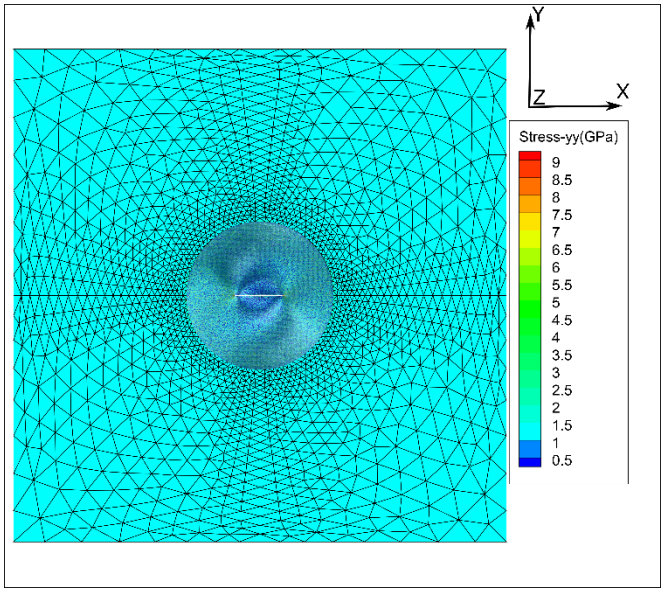

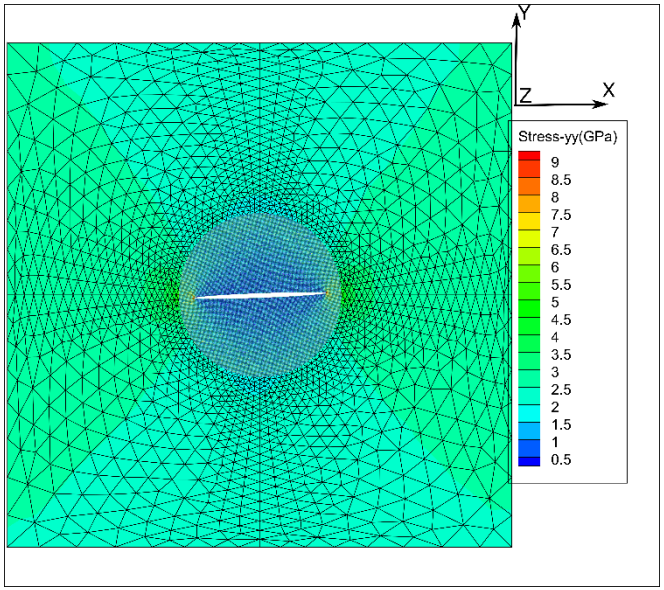

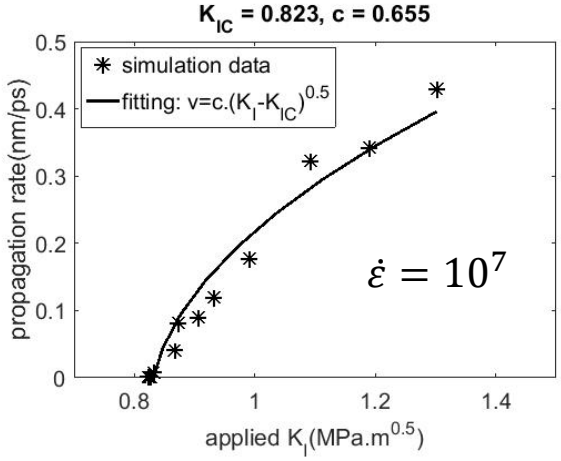

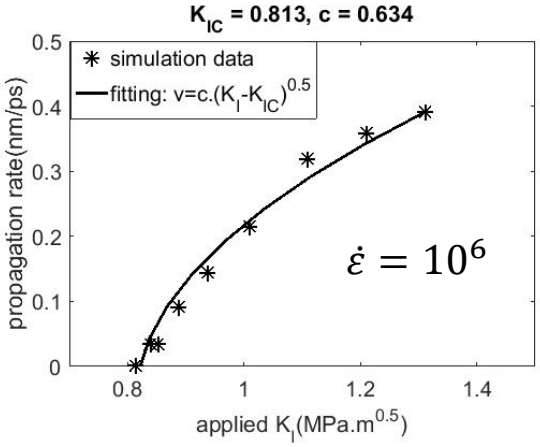

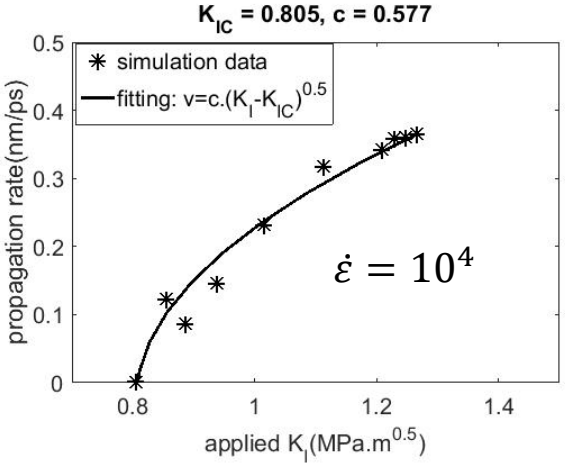

$$v = \dot{a} = \begin{cases} c.(K_I - K_{IC})^{1/2}, & if \;\; K_I > K_{IC} \\ 0, & otherwise \end{cases}$$

Ref: *"Concurrent Atomistic-Continuum Model using Hyperdynamics Accelerated MD Simulations." S. Chakraborty and S. Ghosh, Comp. Mat. Sci. (Accepted).*

Effect of Temperature and Strain Rate on Crack Propagation Rate

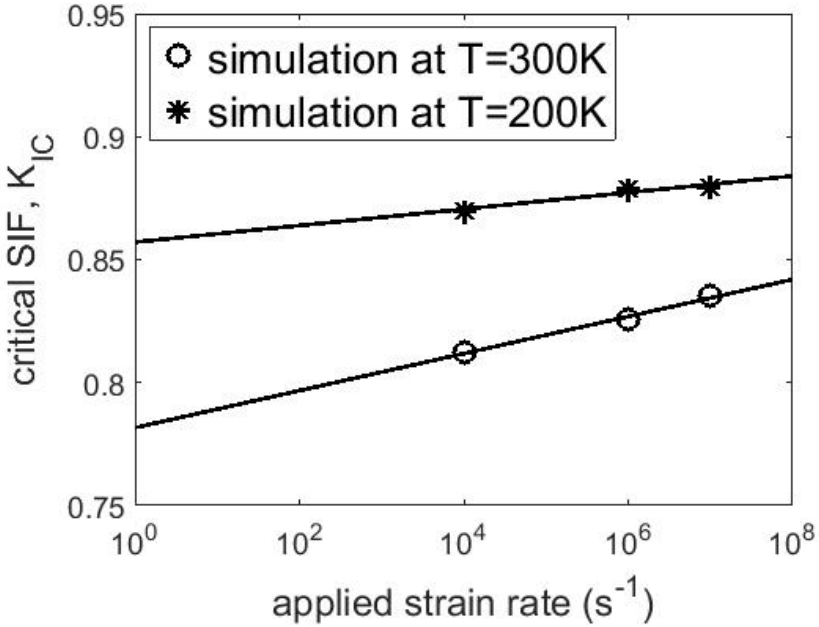

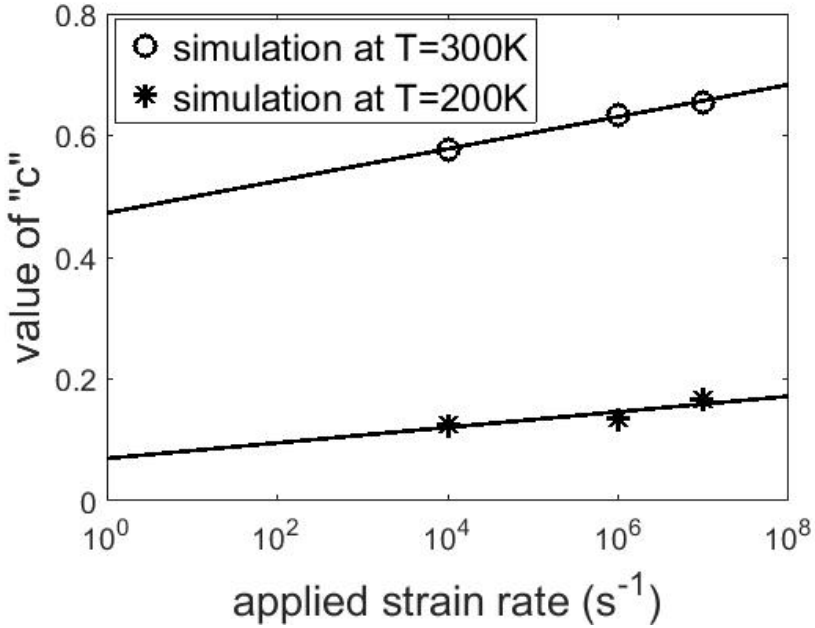

- Parameters corresponding to the evolution of crack have both strain rate and temperature effect on it.
- Temperature effect is more significant than strain rate for the particular orientation used in the present study.

Thermodynamics of Deformation Mechanisms

$$dW = dQ + dU_{el} + dU_{inel} + 2\gamma_s dA = dQ + dU$$

$$dW = \int_{\partial\Omega_c} t.\Delta u^C dA; \quad dQ = 0; \quad dU_{inel} = 0$$

$$dU = \int_{\Omega_c \setminus \Omega_{C_I}} \sigma : \Delta\varepsilon dV + \sum_{p \in \Omega_A \setminus \Omega_{A_I}} \Delta\Phi_p(\bar{r}) + \frac{1}{2}\left[\int_{\Omega_{C_I}} \sigma : \Delta\varepsilon dV + \sum_{p \in \Omega_{A_I}} \Delta\Phi_p(\bar{r})\right]$$

$$2\gamma_s dA = dU - dU_{el}$$

dW : incremental work-potential.

dQ : generated heat.

dU_{el} : incremental recoverable elastic strain-energy.

dU_{inel} : energy due to defects.

γ_s : surface energy density.

dA : increment in crack surface area.

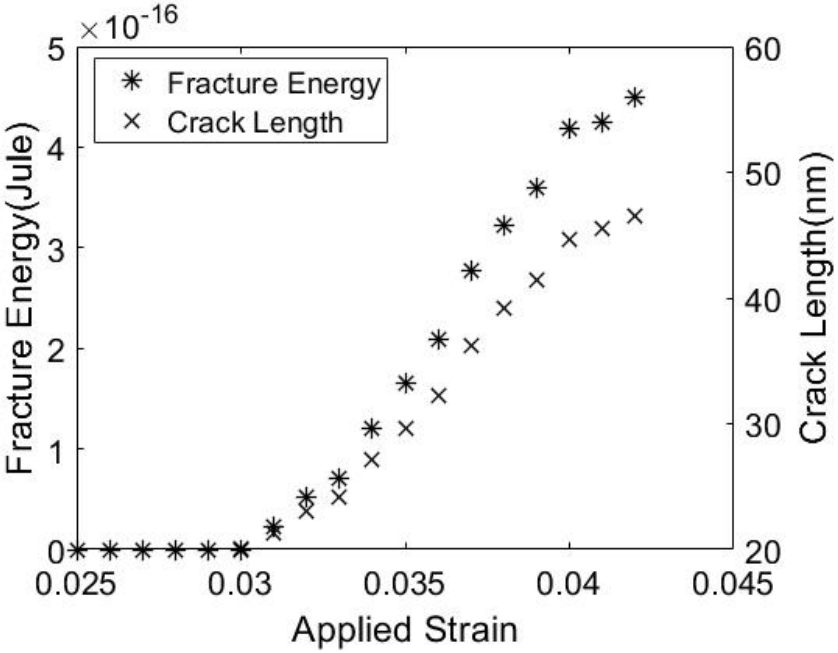

Calibration of Elastic Phase-Field Model Parameter

$$\rho_0\Psi = \frac{1}{2}\tilde{\mathbf{E}}^{\mathbf{e}}:\mathbf{C}^{\mathbf{e}}:\tilde{\mathbf{E}}^{\mathbf{e}} + \frac{g_c}{2l_c}\left(s^2 + l_c^2\Delta_X s.\Delta_X s\right)$$

$$\tilde{E}^e = \frac{1}{2}\left((J^e)^{2/3} - 1\right)\left(g_1(s) - g_2(s)\right)\mathbf{I} + \frac{1}{2}g_2(s)\left(\mathbf{F}^{\mathbf{e}^{\mathbf{T}}}\mathbf{F}^{\mathbf{e}} - \mathbf{I}\right)$$

$$g_1(s) = \begin{cases} 1 & ,J^e < 1 \\ 1 - s & ,otherwise \end{cases}$$

$$g_2(s) = 1 - s$$

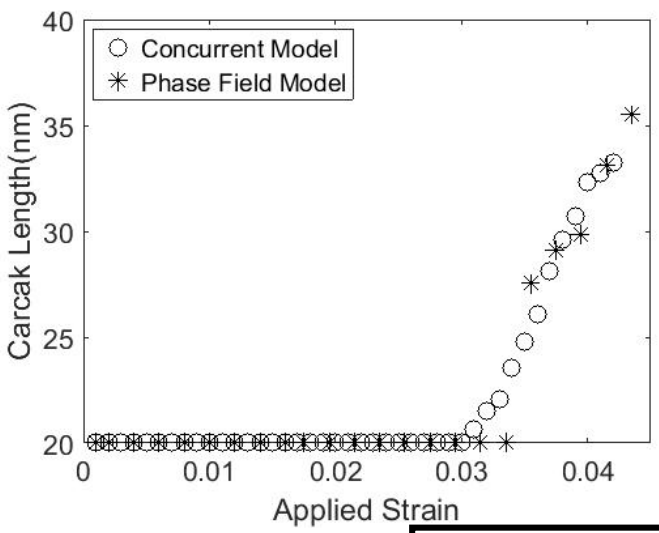

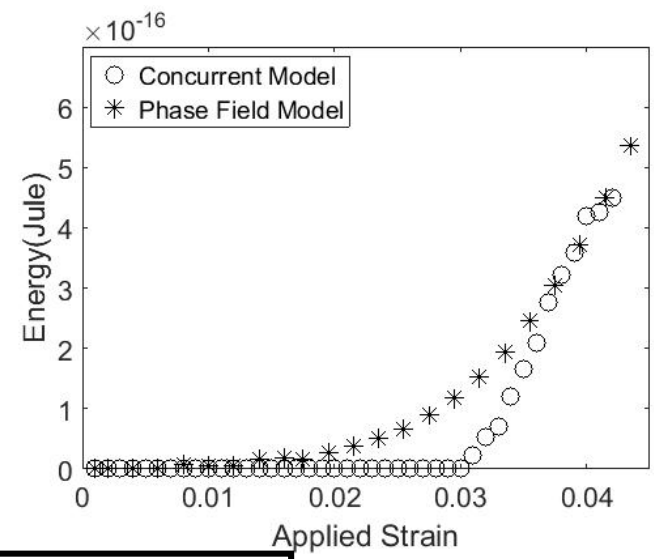

$$\boxed{g_c = 4.6\ \text{Joules/m}^2}$$

Transfer of Dislocation from Atomistic to Continuum Domain

- DXA[1] is used to extract dislocation from atomic data.
- The dislocation is converted into equivalent density form.
- The dislocation is transferred into the continuum in density form.

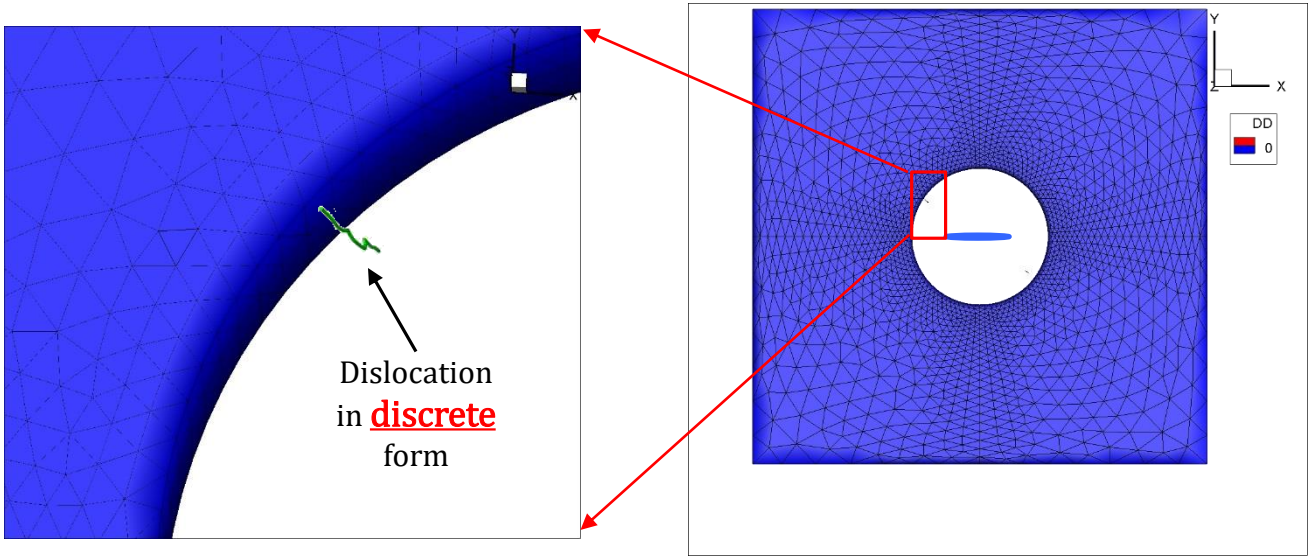

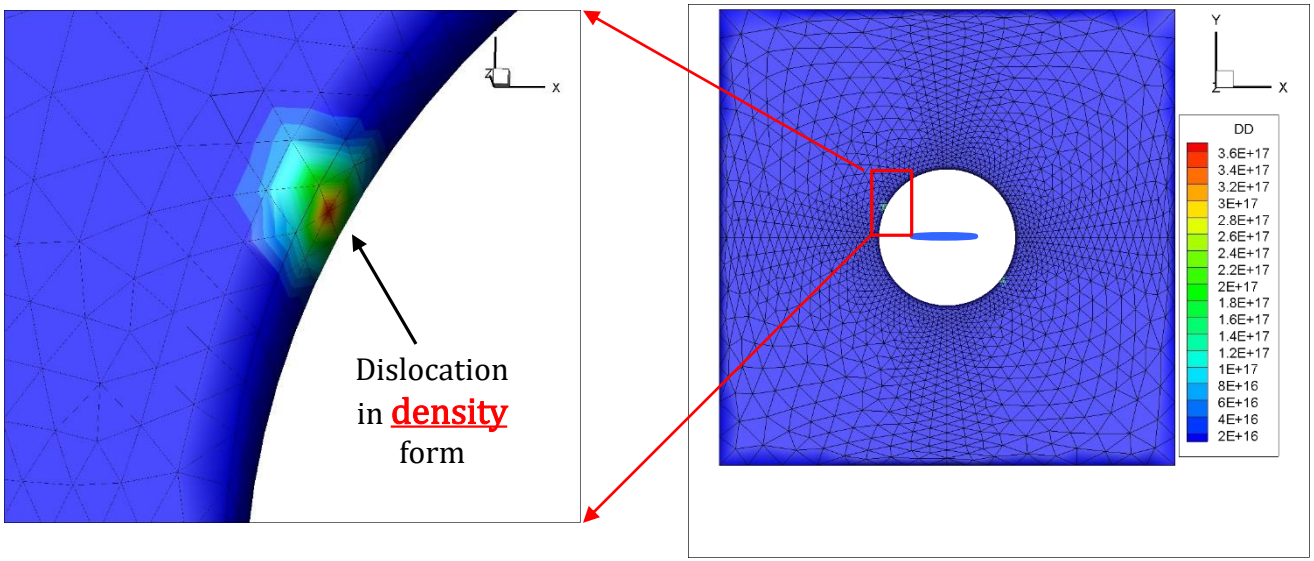

[1] A. Stukowski and K. Able, Modelling Simul. Mater. Sci. Eng. 18:825-847(2010).

Nonlocal Formulation for the Evolution Law of the Incoming Dislocation Flux.

$$\dot{\rho}^{i}_{Flux} = \dot{\rho}^{i}_{FluxGeneration} + \dot{\rho}^{i}_{FluxDepletion}$$

$$\dot{\rho}^{i}_{FluxGeneration} = c_1 \sum_{j=1}^{nNeighbor} \rho^{j}_{Flux} \max\left|0, \left(\hat{d}_{ji} . \hat{v}^{i}\right)\right| \left(e^{\frac{1}{\frac{\left|\bar{d}_{ji}\right|}{a}}}\right) H\left(\left|\tau^{i}\right| - \tau_{pass}\right)$$

$$\dot{\rho}^{i}_{FluxDepletion} = c_2 \sum_{j=1}^{nNeighbor} \rho^{i}_{Flux} \min\left|0, \left(\hat{d}_{ji} . \hat{v}^{i}\right)\right| \left(e^{\frac{1}{\frac{\left|\bar{d}_{ji}\right|}{a}}}\right) H\left(\left|\tau^{i}\right| - \tau_{pass}\right)$$

c_1 and c_2 are material parameter.

d_{ji} : distance between i'th Gauss point and it's j'th neighbor.

v^i: is the dislocation velocity.

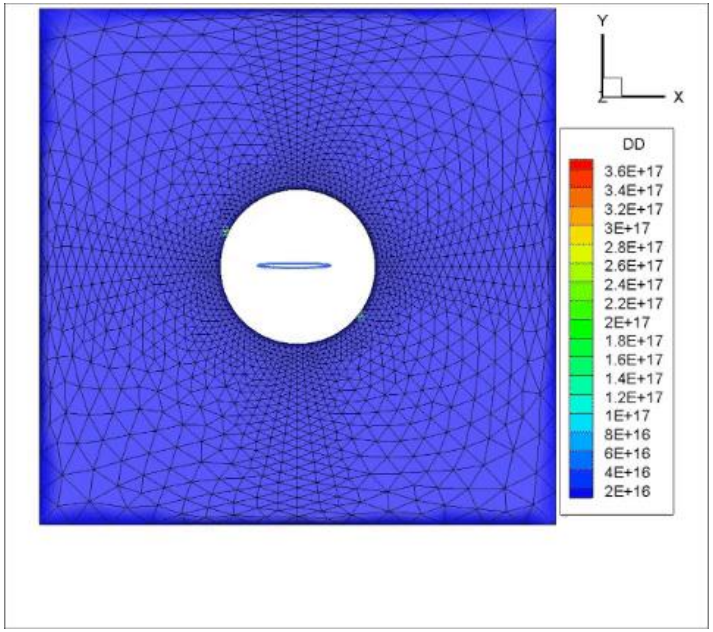

Characterization and quantification of dislocations

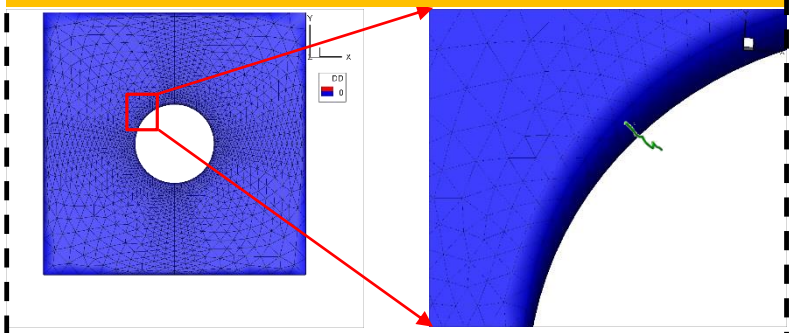

Conversion from discrete to density form

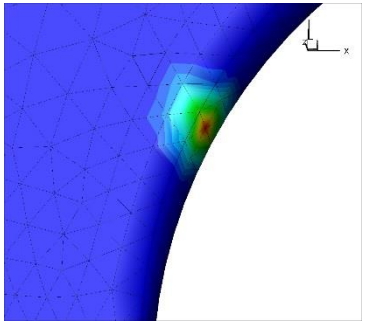

Evolution of Incoming dislocation in continuum

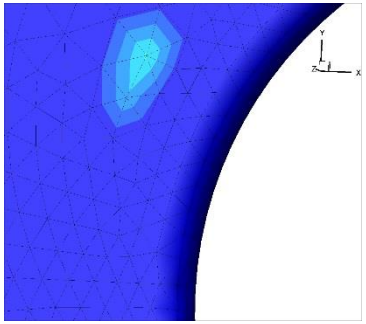

Summary

- Building a Comprehensive Self-Consistent Framework Coupling CPFEM with MD for Crack Evolution models in CPFEM

- Developed robust characterization and quantification methods for deformation mechanism and crack evolution for atomic simulations for transfer of dislocation related variables.

- Hyperdynamics has been used to bridge the time scale difference between atomistic and the continuum domain.

- Extracting phase-field energies from the self consistent model

<u>Ongoing</u>:

- Development of information passing on plasticity when dislocation reaches the interface of $\Omega_{\text{atomistic}}$ and $\Omega_{\text{continuum}}$ and building phase field energies for defect and fracture surfaces